

**NOAA NESDIS
CENTER for SATELLITE APPLICATIONS and
RESEARCH**

ALGORITHM THEORETICAL BASIS DOCUMENT

ABI Ice Cover and Concentration

Yinghui Liu, UW/CIMSS

Jeffrey R. Key, NOAA/NESDIS/STAR

Version 1.03

September 15, 2010

TABLE OF CONTENTS

1	Abstract	7
2	Introduction	7
2.1	Purpose of This Document	7
2.2	Who Should Use This Document	7
2.3	Inside Each Section	8
2.4	Related Documents	8
2.5	Revision History	8
3	Observing System Overview	8
3.1	Instrument Characteristics	8
3.2	Products Generated	9
4	Algorithm Description	10
4.1	Algorithm Overview	10
4.2	Processing Outline	11
4.3	Algorithm Input	13
4.3.1	<i>Primary Sensor Data</i>	13
4.3.2	<i>Ancillary Data</i>	13
4.4	Theoretical Description	13
4.4.1	<i>Physics of the Problem</i>	13
4.4.1.1	<i>Ice and snow reflectance</i>	14
4.4.1.2	<i>Ice surface temperature</i>	14
4.4.2	<i>Mathematical Description</i>	15
4.4.2.1	<i>Ice detection</i>	15
4.4.2.2	<i>Ice concentration from tie points algorithm</i>	16
4.4.2.3	<i>Ice Cover</i>	18
4.4.3	<i>Algorithm Output</i>	18
5	Test Data Sets and Validations	20
5.1	Simulated Input Data Sets	20
5.1.1	<i>MODIS Data</i>	21
5.1.2	<i>SEVIRI Data</i>	23
5.2	Output from Simulated Inputs Data Sets	24
5.2.1	<i>Precisions and Accuracy Estimates</i>	24
5.2.1.1	<i>Comparison with the AMSR-E product</i>	24
5.2.1.2	<i>Comparison with the satellite true color images</i>	25
5.2.2	<i>Error Budget</i>	26
6	Practical Considerations	28
6.1	Numerical Computation Considerations	28
6.2	Programming and Procedural Considerations	28
6.3	Quality Assessment and Diagnostics	28
6.4	Exception Handling	28
6.5	Algorithm Validation	28
7	Assumptions and Limitations	29
7.1	Assumptions	29

7.2	Limitations	29
7.3	Pre-Planned Product Improvements	30
8	References	31

LIST OF FIGURES

Figure 1. High Level Flowchart of the ice cover and concentration algorithm illustrates the Main Processing Sections.....	12
Figure 2a. Reflectance probability density distribution at 0.64 μm for ice cover over Lake Erie on Feb 24 th , 2008.	17
Figure 2b. Reflectance probability density distribution at 0.64 μm for ice cover over Barents and Kara Seas on Mar 31 st , 2008.	18
Figure 3. Sea ice concentration (%) retrieved from (a) MODIS Sea Ice Temperature (SIT), (b) MODIS visible band (0.64 μm) reflectance using tie points algorithm on March 31 st 2006.	22
Figure 4. Lake ice concentration (%) with MODIS Aqua visible band (0.64 μm) data on February 24 2008.	22
Figure 5. MSG Telecommunications coverage area.....	23
Figure 6. Lake ice concentration (%) retrieved from (a) SEVIRI Surface Ice Temperature (SIT), (b) SEVIRI visible band reflectance (0.64 μm) on January 27 th , 2006.	24
Figure 7. Sea ice concentration (SIC) (%) retrieved from (a) MODIS Sea Ice Temperature (SIT), (b) MODIS visible band reflectance, and (c) from Advanced Microwave Scanning Radiometer - Earth Observing System (AMSR-E) Level-3 gridded daily mean from NSIDC on March 31 st , 2006.....	25
Figure 8. Lake ice concentration (%) retrieved from (a) SEVIRI Surface Ice Temperature (SIT), (b) SEVIRI visible band reflectance (0.64 μm), and (c) satellite true color image over Caspian Sea on January 27 th , 2006.	26
Figure 9. Lake ice concentration (%) with MODIS Aqua data (left, MODIS true color image (middle), and ice concentration from AMSR-E (right) over Great Lakes on February 24 2008.	26
Figure 10. Frequency distribution of ice concentration difference between AMSRE product and retrievals using this algorithm based on selected 41 clear day MODIS data in four seasons in 2007 over the Arctic Ocean.	27

LIST OF TABLES

Table 1. Product Function and Performance Specification for ice cover.....	9
Table 2. Product Function and Performance Specification for ice cover.....	9
Table 3. Summary of the Current ABI Channel Numbers and Wavelengths.	10
Table 4. Values of coefficients a, b, c, and d in equation (1) for MODIS	15
Table 5. Output and additional output parameters and their definitions.....	18
Table 6. Ice Cover and Concentration Quality Information (4 bytes)	18
Table 7. Channels in the proxy data associated with GOES-R ABI.	21
Table 8: Performance of ice cover product	27
Table 9. Performance of retrieved ice concentration.	27

LIST OF ACRONYMS

ABI: Advanced Baseline Imager
AIT: Algorithm Integration Team
AMSR-E: Advanced Microwave Scanning Radiometer - Earth Observing System
ATBD: Algorithm Theoretical Basis Document
AWG: Algorithm Working Group
CIMSS: Cooperative Institute for Meteorological Satellite Studies
FOV: Field of View
GOES-R: Geostationary Operational Environmental Satellite R series
MODIS: Moderate Resolution Imaging Spectroradiometer
MRD: Mission Requirements Document
MSG: Meteosat Second Generation
NDSI: Normalized Difference Snow Index
NOAA: National Oceanic and Atmospheric Administration
SEVIRI: Spinning Enhanced Visible and Infrared Imager
TOA: Top Of the Atmosphere

1 Abstract

The cryosphere exists at all latitudes and in about one hundred countries. It has profound socio-economic value due to its role in water resources and its impact on transportation, fisheries, hunting, herding, and agriculture. It also plays a significant role in climate studies, and understanding the cryosphere is critical for accurate weather forecasts. Among the properties of the cryosphere, ice cover and ice concentrations are the most important. This document provides high level description of the physical basis and technical approach of the algorithms to identify ice cover and estimate ice concentration over water surfaces for clear pixels with supplementary information from observations and products retrieved from the Advanced Baseline Imager (ABI) on the Geostationary Operational Environmental Satellite R series (GOES-R) of the National Oceanic and Atmospheric Administration's (NOAA) geostationary meteorological satellites. Group threshold methods are applied on observations from visible and infrared bands to identify ice cover over water surfaces under clear sky conditions; a tie-point algorithm is used to determine the representative reflectance/temperature of the 100% ice covered surface, which is in turn applied to estimate the ice concentration. The algorithm is tested extensively using other satellite observations as proxy data for the GOES-R ABI. Validations show that the results meet the requirements for product measurement accuracy and precision.

2 Introduction

2.1 Purpose of This Document

This algorithm theoretical basis document (ATBD) provides a high level description of the physical basis and technical approach for identifying ice cover and estimating ice concentration over water surfaces for clear pixels with supplementary information from observations and products retrieved from the Advanced Baseline Imager (ABI) on the Geostationary Operational Environmental Satellite R series (GOES-R) of the National Oceanic and Atmospheric Administration's (NOAA) geostationary meteorological satellites. This ice cover and concentration algorithm is designed to identify ice over water surfaces including frozen inland lakes and rivers, and oceans, and to provide estimations of ice concentration, noted as fractions (in tenths) of the sea or lake surface covered by ice, for each ABI pixel identified as ice over water surfaces. No land ice applications are included. Output of this algorithm is available to other algorithms, which require knowledge of the ice information. The ice information is also important for planning commercial transportation, short-term weather forecasting, water management, and damage control. Long-term records of ice cover and concentration data are valuable for climate change studies.

2.2 Who Should Use This Document

The intended users of this document are those interested in understanding the physical basis and technical approach of the algorithm, and applying the output of this algorithm for a particular

purpose. This document also provides information useful to anyone to implement, maintain and improve the original algorithm.

2.3 Inside Each Section

This document is broken down into the following main sections.

- **System Overview:** Provides relevant details of the ABI, and a brief description of the products to be generated by this algorithm.
- **Algorithm Description:** Provides the detailed description of the algorithm including its physical basis, technical approach, and required input, and output.
- **Assumptions and Limitations:** Provides an overview of the assumptions, limitations of the current approach and future plans to overcome these limitations.

2.4 Related Documents

This document currently does not relate to any other document outside of the specifications of the GOES-R Mission Requirements Document (MRD) and to the references given through out.

2.5 Revision History

Version 0.0 of this document was created by Yinghui Liu of the Cooperative Institute for Meteorological Satellite Studies (CIMSS), University of Wisconsin-Madison, and Jeffrey R. Key of NOAA/NESDIS/STAR, and is intended to accompany the delivery of the version 0.0 algorithms to the GOES-R Algorithm Working Group (AWG) Algorithm Integration Team (AIT). Version 1.0 is for the 80% ready ATBD submitted to the Algorithm Integration Team (AIT).

3 Observing System Overview

This section describes characteristics of ABI, as well as the products generated by the ABI ice cover and concentration algorithm.

3.1 Instrument Characteristics

The ABI onboard the future GOES-R has a wide range of applications in weather, oceanographic, climate, and environmental studies. ABI has 16 spectral bands (Table 1), with visible bands, 5 near-infrared bands, and 9 infrared bands. The spatial resolution of ABI will be nominally 2 km for the infrared bands, 1 km for the 0.47, 0.86, and 1.61 μm bands, and 0.5 km for the 0.64 μm visible band. ABI will scan the full disk every 15 minutes, the continental United States 3 times, plus a selectable 1000 km \times 1000 km area every 30 s. ABI can also be

programmed to scan the full disk every 5 minutes. Compared to the current GOES imager, ABI offers more spectral bands and higher spatial resolution. In particular, the newly added band at 1.61 μm and the higher spatial resolution at 0.64 μm allow for better detection and monitoring of surface snow and ice (Schmit et al., 2005).

3.2 Products Generated

The ice cover and concentration algorithm is responsible for identifying all ABI pixels covered with ice over water surfaces under clear conditions, as well as estimating ice concentration. No land ice applications are included. In terms of the GOES-R MRD, ice cover reports the location of ice over frozen inland lakes, rivers, and open waters, and ice concentration reports the fraction (in tenths) of the sea or lake surface covered by ice. Total concentration includes all ice types that are present. The required product Function and Performance Specification (F&PS) for ice cover and ice concentration are listed in Tables 1 and 2 respectively.

Table 1. Product Function and Performance Specification for ice cover.

Name	Ice Cover
User and Priority	GOES-R
Geographic Coverage (G, H, C, M)	FD
Vertical Resolution	N/A
Horizontal Resolution	2km
Mapping Accuracy	1km
Measurement Range	Binary yes/no detection
Measurement Accuracy	85% correct detection
Product Refresh Rate/Coverage Time	180 min
Vendor Allocated Ground	77,756 sec
Product Measurement Precision	N/A

Table 2. Product Function and Performance Specification for ice concentration.

Name	Sea & Lake Ice Concentration	Sea & Lake Ice Concentration
User and Priority	GOES-R	GOES-R
Geographic Coverage (G, H, C, M)	C: Regional and Great Lakes and US costal waters containing sea ice hazards to navigation	FD: Sea ice covered waters in N & S Hemisphere
Vertical Resolution	Ice Surface	Ice Surface
Horizontal Resolution	3 km	10 km
Mapping Accuracy	≤ 1.5 km	≤ 5 km
Measurement Range	Ice concentration 1/10 to 10/10	Ice concentration 1/10 to 10/10
Measurement Accuracy	10%	10%

Product Refresh Rate/Coverage Time	180 min	6 hr
Vendor Allocated Ground	3236 sec	9716 sec
Product Measurement Precision	30%	30%

Ice cover will be produced for each ABI pixel over a water surface, and ice concentration will be calculated for each pixel covered with ice. Both products are for pixels under clear-sky condition only. Observations needed in this algorithm include reflectance at the Top Of the Atmosphere (TOA) with viewing angle correction in ABI channel numbers 2, 3, 5, and brightness temperatures in ABI channel numbers 14 and 15.

Table 3. Summary of the Current ABI Channel Numbers and Wavelengths.

<i>Channel Number</i>	<i>Wavelength (μm)</i>	<i>Subsatellite Field of View (km)</i>	<i>Direct Use in AITA</i>
1	0.47	1	No
2	0.64	0.5	Yes
3	0.86	1	Yes
4	1.38	2	No
5	1.61	1	Yes
6	2.26	2	No
7	3.9	2	No
8	6.15	2	No
9	7.0	2	No
10	7.4	2	No
11	8.5	2	No
12	9.7	2	No
13	10.35	2	No
14	11.2	2	Yes
15	12.3	2	Yes
16	13.3	2	No

This algorithm relies on the accuracy of other products including cloud mask, land/water mask, etc. Details of the required input parameters and current validations are presented in the following sections. An algorithm sensitivity study will be reported in the next version.

4 Algorithm Description

A complete description of the algorithm is presented at its current level of maturity. The algorithm will be updated with each revision.

4.1 Algorithm Overview

This automated algorithm detects the ice cover and retrieves the ice concentration. Ice cover is first determined by a group-criteria technique. Then the ice concentration is retrieved by applying a tie point algorithm on each ice-covered pixel. Ice cover is further refined based on the retrieved ice concentration.

Pros:

- This automated algorithm is designed on a solid physical foundation, and is capable of retrieving ice cover and concentration for both day and nighttime.
- It runs automatically, and can be employed globally.

Cons:

- The accuracy of this algorithm depends on the quality of the cloud mask, and no retrieval can be carried out for cloudy pixels.

4.2 Processing Outline

The processing outline of this algorithm is summarized in the following chart.

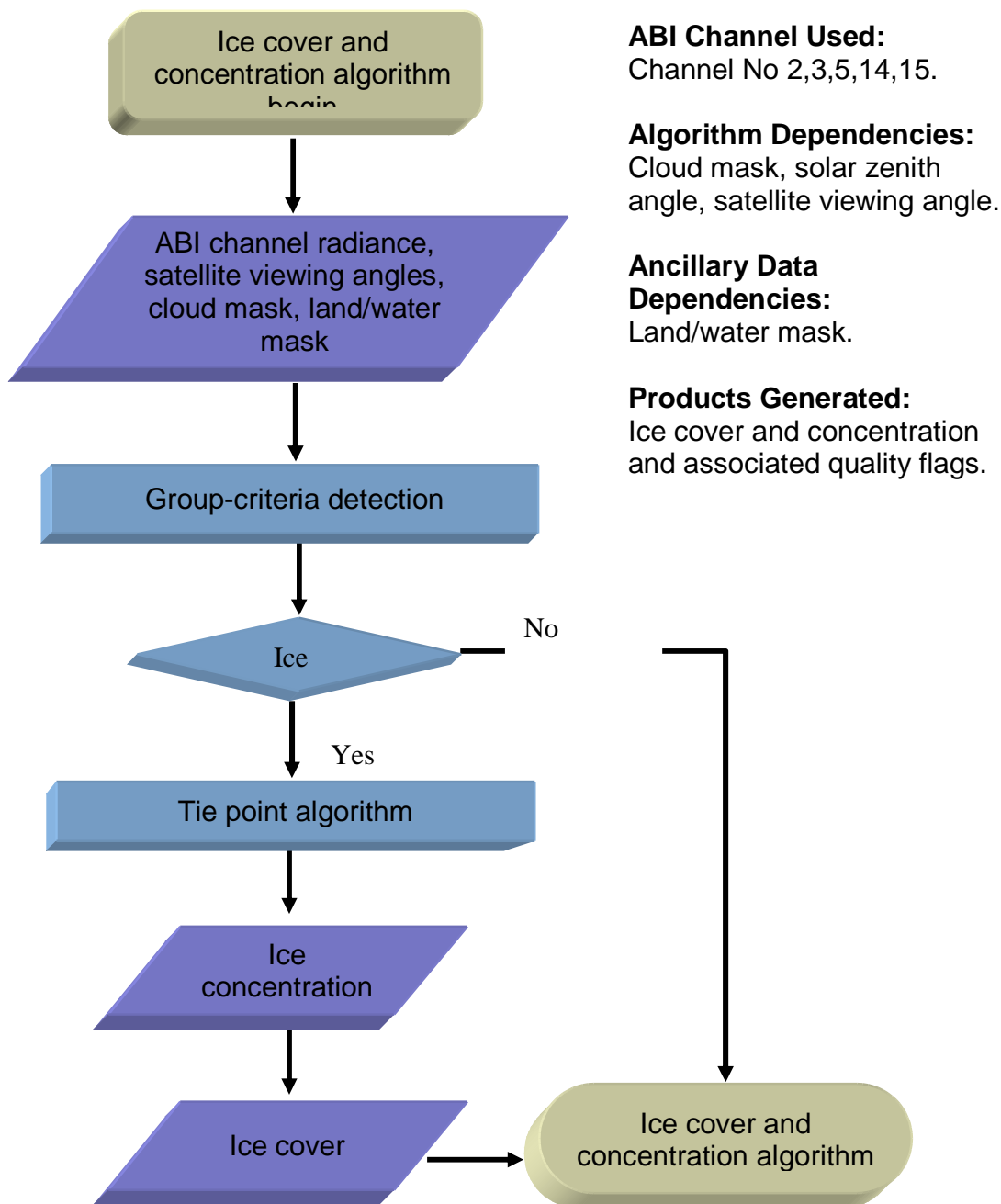


Figure 1. High Level Flowchart of the ice cover and concentration algorithm illustrates the Main Processing Sections.

4.3 Algorithm Input

This section describes the input of the ice cover and concentration algorithm.

4.3.1 Primary Sensor Data

The list below contains the primary parameter data used in this algorithm. Primary parameter data represents information that are derived mainly from the ABI observations and geo-location information.

- **Reflectance in ABI channels 2, 3, and 5**
- **Brightness temperature in ABI channels 14 and 15**
- **Derived ABI cloud mask**
- **Derived surface skin temperature using this algorithm**
- **Sensor viewing zenith angle**
- **Solar zenith angle**
- **Longitude, latitude**

4.3.2 Ancillary Data

The following list notes the ancillary data required in this algorithm. Ancillary data represents data that requires information not included in the ABI observations or geo-location data.

- **Land mask**
- **Coast mask**

4.4 Theoretical Description

Sea and lake ice influence the surface radiation budget, and affect energy and moisture exchange between the atmosphere and the underlying water, leading them to be one of the key factors to consider in atmospheric circulation, numerical weather forecasting, and climate models. While ice cover is important for planning commercial transport, ice cover and concentration are among the most important indices in studying climate change. Accurate retrievals of ice cover and concentration are of high importance both to the scientific communities and to the public.

Physical and statistical approaches are applied to determine sea and lake ice cover and to estimate the ice concentration. In the following sections, the physical background and technical approaches of the processes in this algorithm are described.

4.4.1 Physics of the Problem

4.4.1.1 Ice and snow reflectance

Ice reflectance depends strongly on its internal structure, such as brine pockets or air bubbles of the near surface layers. These internal structures change with season, state of the near surface layers, and age of the ice, which results in different ice types. Ice surface reflectance is different from snow surface reflectance. Ice consists mainly of sheets, while snow consists of grains. Absorption and scattering in the snow and ice cover are determined by their internal inhomogeneities (Grenfell and Maykut, 1977). Snow reflectance shows very high values at visible channels, but low values at short-wavelength channels longer than 1.4 microns (Bolsenga 1983), due to the much stronger absorption and much less back scattering at those infrared channels. This feature is shared by snow-covered ice and many ice types. Most of the ice surfaces show higher reflectance at visible and near infrared channels than water surfaces, which can be used to detect ice cover. Other substances do not have this unique spectral signature of snow and ice. Clouds have high reflectance at both visible and near infrared channels while water surfaces are dark at all wavelengths (Riggs et al. 1999). However, some ice types, such as clear lake ice and grease ice, can be difficult to detect due to their very low contrast with open water.

4.4.1.2 Ice surface temperature

Ice surface temperature is retrieved using brightness temperatures from GOES-R ABI channel numbers 14 and 15 with center wavelengths at 11.2, and 12.3 μm , and the satellite sensor scan angle derived from the sensor zenith angle. The retrieval algorithm is from the work of Key et al. (1997). To retrieve ice/snow surface skin temperature (IST), the following equation is used.

$$T_s = a + bT_{11} + cT_{12} + d [(T_{11}-T_{12})(\sec \theta - 1)] \quad (1)$$

where T_s is the estimated surface skin temperature (K), T_{11} and T_{12} are the brightness temperatures (K) at the 11 μm and 12 μm bands, and θ is the sensor scan angle. Coefficients a , b , c , and d are derived for the following temperature ranges: $T_{11} < 240\text{K}$, $240\text{K} < T_{11} < 260\text{K}$, $T_{11} > 260\text{K}$. The coefficients are based on modeled radiances in the 11 and 12 μm bands using Arctic and Antarctic temperature and humidity profiles, and angular emissivity models for snow. The equations do not include a bias term to account for differences between modeled and actual radiances. This bias term has not been necessary for NOAA-14, which was validated extensively with surface data from the SHEBA experiment. It may or may not be necessary for other platforms, e.g. GOES-R ABI. See Key et al. (1997) for additional details. The coefficients were updated for the Moderate Resolution Imaging Spectroradiometer (MODIS) onboard the Terra and Aqua satellites (see the values of these coefficients for MODIS in Table 2), and for the Spinning Enhanced Visible and Infrared Imager (SEVIRI) onboard the Meteosat Second Generation (MSG) satellites, and will be updated for GOES-R ABI. In equation (1), the sensor scan angle is derived from the sensor zenith angle using equation (2).

$$\theta = \arcsin(\sin(\lambda) \times R_e / (R_e + A_{sat})) \quad (2)$$

where λ is the sensor zenith angle, R_e is the equatorial radius of the Earth, and A_{sat} is the nominal altitude of the satellite.

This method is specifically designed for retrievals over ice/snow surfaces, which is not provided from the land team.

Table 4. Values of coefficients a , b , c , and d in equation (1) for MODIS

Temperature Range	a	b	C	d
< 240 K	-0.159480	0.999926	1.390388	-0.413575
240 – 260 K	-3.329456	1.012946	1.214573	0.131017
> 260 K	-5.207360	1.019429	1.510250	0.260355

4.4.2 Mathematical Description

4.4.2.1 Ice detection

Ice cover is detected at the pixel level over water surfaces under clear conditions. Clear conditions are determined from the cloud mask.

Snow covered ice shows high reflectance in the visible channels, and very low reflectance in short-wavelength infrared channels. Many ice types also have this characteristic, and most ice types have higher reflectance than open water, which typically has a very low reflectance.

Traditionally, Normalized Difference Snow Index (NDSI) is used to detect snow and ice. NDSI is defined as

$$NDSI = (R_1 - R_2) / (R_1 + R_2) \quad (3)$$

where R_1 is often the reflectance in the visible channel, (e.g., 0.55 μm for MODIS), R_2 is the reflectance in the short-wavelength infrared channel (e.g., 1.6 or 2.1 μm for MODIS). Ice is identified when NDSI is larger than a preset threshold. For GOES-R ABI, channel number 3 (0.865 μm), and channel number 5 (1.61 μm) are selected to calculate NDSI. Both channels have the same spatial resolution (1km at sub-satellite Field of View (FOV)). Furthermore, one advantage of 0.865 μm over 0.55 μm to calculate NDSI is that NDSI calculated using 0.55 μm reflectance is higher than the preset threshold over water surfaces in some cases, while NDSI from 0.865 μm is mostly lower than the preset threshold.

In the daytime (solar zenith angle lower than 85 degrees), a pixel is identified as possible ice if the NDSI value is larger than 0.6, the reflectance at GOES-R ABI channel number 3 (0.865 μm) is higher than 0.08 (Hall et al. 2001, 2006), and the surface temperature is lower than preset thresholds (273 K over fresh water, and 271.0 K over ocean).

Ice cover has a colder surface temperature than open water, and water with higher salinity usually has a lower melting temperature. During the nighttime (solar zenith angle higher than or equal to 85 degrees), a pixel is identified as possible ice if the surface temperature is lower than 273.0 K over lakes, or lower than 271.0 K over ocean (salty) water.

4.4.2.2 Ice concentration from tie points algorithm

Ice characteristics change temporally and spatially. Different ice types can appear simultaneously in a large field of view, and change over time. Under certain conditions when a single ice type appears in a search window with a certain shape and size, the surface reflectance or temperature of the pure ice is homogeneous, as well as different from open water. Changes in surface reflectance/temperature at the pixel level are mainly due to different ice concentrations, the fraction of the surface covered by ice. Theoretically, the reflectance and temperature of pure ice and open water can be derived from a tie point method, if 100% ice covered pixels are the majority in each search window, e.g., a square or a circle. (Figures 2a, 2b).

Then, ice concentration for a pixel (F_p) inside the search window can be calculated by

$$F_p = (B_p - B_{water}) / (B_{ice} - B_{water}) \quad (4)$$

where B_{water} is the reflectance/temperature of pure water pixels and B_{ice} is the reflectance/temperature of pure ice pixels; B_p is the observed reflectance/temperature of the pixel, from which ice concentration will be calculated. In this algorithm, the reflectance from GOES-R ABI channel number 2 (0.64 μm) is selected in the daytime, and the surface skin temperature is selected both in daytime and in nighttime. Whether the final ice concentration in the daytime uses only the retrievals from the reflectance, or only the retrievals from the surface skin temperature, or the optimal combination of both retrievals is under consideration. The spatial resolution is 0.5 km for the 0.64 μm channel, and 2.0 km for the surface temperature at the sub-satellite FOV.

Determining the reflectance/temperature of pure ice pixels is the key to calculate the ice concentration. In a search window that is 50 pixels \times 50 pixels, the ice reflectance/temperature probability density function (PDF) is calculated using all the possible ice pixels detected in the first step described in section 3.4.2.1. This PDF is presented as histogram bins. For the reflectance, the minimum bin value is 0, with a bin width of 0.02, and a total bin number of 90. For temperature, the minimum bin value is 230 K, with a bin width of 0.5 K, and a total bin number of 90. The histogram bins are then smoothed by a running boxcar filter that is 5 bins in size, in which a sliding integral is calculated over the original PDF. As a result, a new smoothed PDF is derived. The ice reflectance/temperature tie point is chosen as the reflectance/temperature, with the maximum probability density in the smoothed PDF, or with the maximum sliding integral. The tie point reflectance of open water is a function of solar zenith angle, with 0.05 for solar zenith angles less than 65 degrees and 0.07 for solar zenith angles equal to or larger than 65 degrees. The tie point surface temperature of open water changes with the water salinity, 273.0 K for fresh water and 271.0 K for salty water. The tie point algorithm described above is adapted from a similar algorithm by Appel and Jensen (2002). The reason that the location of the max PDF point is selected as the tie point with 100% ice concentration is that

ice with 100% ice concentration is assumed to be the majority in a search window, and that the ice characteristics are homogeneous in the search window.

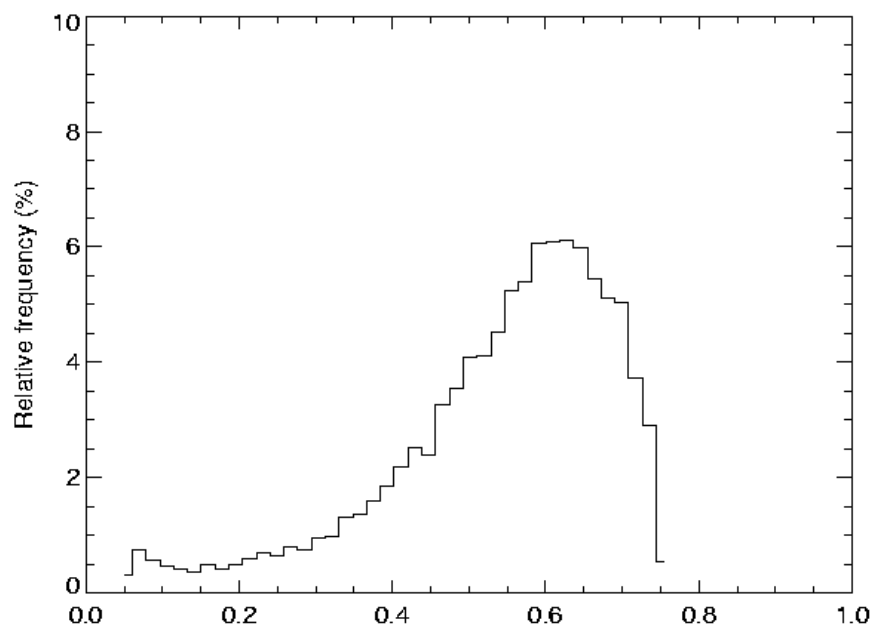


Figure 2a. Reflectance probability density distribution at $0.64 \mu\text{m}$ for ice cover over Lake Erie on Feb 24th, 2008.

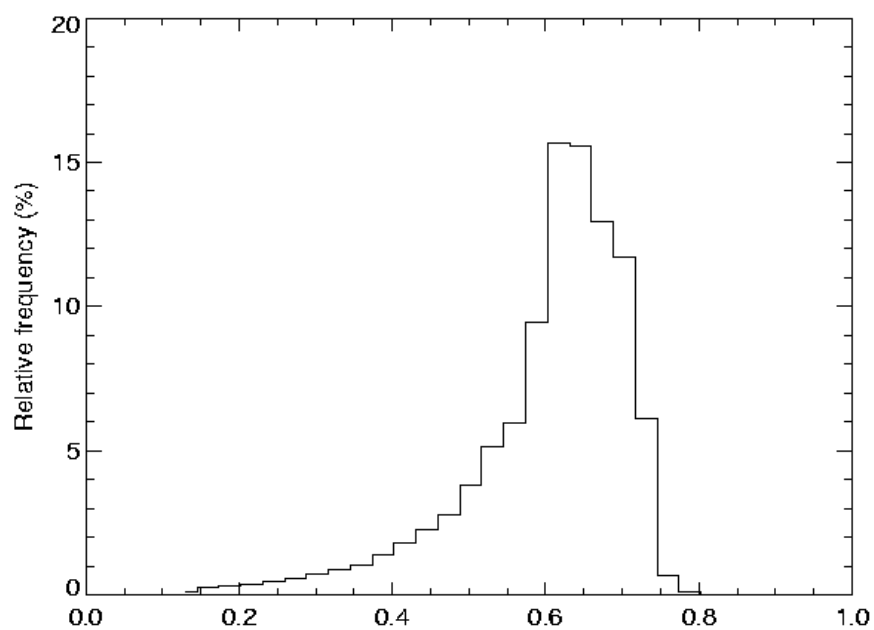


Figure 2b. Reflectance probability density distribution at 0.64 μm for ice cover over Barents and Kara Seas on Mar 31st, 2008.

4.4.2.3 Ice Cover

Ice cover is first determined after ice detection tests, and refined with retrieved ice concentration. As the first step, pixels with ice detected at daytime are assigned a value of 1, and assigned a value of 2 at nighttime when only the surface skin temperature test is used. Pixels covered with water are assigned a value of 3. After the ice concentration is retrieved, ice pixels determined after the first step are assigned a value of 3 (water surface) if the retrieved ice concentration is less than 15%.

4.4.3 Algorithm Output

The outputs of this algorithm are ice cover and ice concentration (Table 3) along with other optional parameters and associated quality flags (Table 4).

Table 5. Output and additional output parameters and their definitions.

Definition	Description
Ice concentration	The fraction (in tenths or percentage) of the sea or lake surface covered by ice
Ice cover	A pixel is ice covered or not. Value 1: ice detected using daytime tests 2: ice detected using nighttime tests 3: water surface 4: non-retrievable due to cloud cover
Ice surface temperature (additional)	Skin temperature at ice surface.

Table 6. Ice Cover and Concentration Quality Information (4 bytes)

Byte	Bit	Quality Flag Name	Description	Meaning
0	0	QC_otuput	Output product quality	00 - normal
	1			01 - uncertain
	2	QC_INPUT_CLD	Input cloud mask	10 - non-retrievable
	3			11 - bad data
	4			00 - clear
	5	QC_INPUT_DAY	Day/Night	01 - probably clear
	6	QC_INPUT_SUNGLINT	Sunglint or not	10 - probably cloudy
7	QC_INPUT_CLDSHADOW	Cloud shadow or not	11 - cloudy	
1	0	empty		0-Day 1-Night
		QC_INPUT_SOLZEN	Valid solar zenith angle	0-Yes 1-No

	1	QC_INPUT_SATZEN	Valid satellite zenith angle	0-Yes 1-No
	2	QC_INPUT_REFL	Valid ABI reflectance at band 1	0-Yes 1-No
	3		Valid ABI reflectance at band 2	0-Yes 1-No
	4		Valid ABI reflectance at band 3	0-Yes 1-No
	5		Valid ABI reflectance at band 5	0-Yes 1-No
	6	QC_INPUT_THERMAL	Valid ABI brightness temperature at band 14	0-Yes 1-No
	7		Valid ABI brightness temperature at band 15	0-Yes 1-No
2	0	QC_INPUT_SURFACE	Surface background flag	00 - in-land water 01 - sea water 10- land 11 - others
	1			
	2	QC_TEST_REFL	Reflectance test	0-Yes 1-No
	3	QC_TEST_NDSI	NDSI test	0-Yes 1-No
	4	QC_TEST_SKINTEMP	Skin temperature test	0-Yes 1-No
	5	QC_TIE_REFL	Visible band tie-point algorithm	0-Yes 1-No
	6	QC_TIE_SKINTEMP	Skin temperature tie-point algorithm	0-Yes 1-No
	7	empty		
3	0			
	1			
	2			
	3			
	4			
	5			
	6			
	7			

File metadata are also included in the final product. The metadata include the common metadata for all data products and specific metadata for ice cover and concentration product.

Common metadata for all data products:

- DateTime (swath beginning and swath end)
- Bounding Box
 - Product resolution (nominal and/or at nadir)
 - Number of rows, and number of columns
 - Bytes per pixel
 - Data type
 - Byte order information
 - Location of box relative to nadir (pixel space)
- Product Name
- Product units
- Ancillary data to produce product (including product precedence and interval between datasets is applicable)
 - Version Number

- Origin
- Name
- Satellite
- Instrument
- Altitude
- Nadir pixel in the fixed grid
- Attitude
- Latitude, longitude
- Grid projection
- Type of scan
- Product version number
- Data compression type
- Location of production
- Citations to documents
- Contact information

Ice Cover and Concentration Specific Metadata:

- Number of QA flag values (currently, there are 4: Normal or Optimal; Uncertain or Suboptimal; Non-retrievable; Bad data)
- For each QA flag value, the following information is provided:
 - Definition of QA flag
 - Total pixel numbers with the QA flag
- Total number of pixels with water surface
- Total number of valid ice cover and concentration retrievals (normal+uncertain)
- Total percentage of valid ice cover and concentration retrievals of all pixels with water surface
- Total pixel numbers and percentage of terminator pixels (Non-retrievable and Bad data)
- Number of pixels for valid daytime ice cover and concentration retrievals
- Number of pixels for valid nighttime ice cover and concentration retrievals
- Mean, Min, Max, and standard deviation of valid ice concentration retrievals
- Pixel size of search window to determine tie-point.

5 Test Data Sets and Validation

5.1 Simulated Input Data Sets

The GOES-R ABI proxy data used to test this algorithm included observations from MODIS and the Spinning Enhanced Visible & InfraRed Imager (SEVIRI) onboard of the MSG (Meteosat Second Generation) satellites. The channels in the proxy data associated with the GOES-R ABI are listed in Table 7. Validations were performed by comparison to passive microwave ice cover and concentration product from the Advanced Microwave Scanning Radiometer - Earth Observing System (AMSR-E) observations, and comparison with true-color satellite images detailed in the following subsections. Our testing and validations include both sea and lake ice.

Table 7. Channels in the proxy data associated with the GOES-R ABI.

<i>ABI Channel Number</i>	<i>ABI Wavelength (μm)</i>	<i>MODIS band v (Wavelength μm)</i>	<i>SEVIRI band (Wavelength μm)</i>
2	0.64	1 (0.64)	1 (0.635)
3	0.86	2 (0.86)	2 (0.81)
5	1.61	6 (1.6)	3 (1.64)
14	11.2	31 (11)	9 (10.80)
15	12.3	32 (12)	10 (12.0)

5.1.1 MODIS Data

MODIS (Moderate Resolution Imaging Spectroradiometer) is a key instrument aboard the Terra (*EOS AM*, refer to <http://terra.nasa.gov/>) and Aqua (*EOS PM*, refer to <http://aqua.nasa.gov/>) satellites. Terra's orbit around the Earth is timed so that it passes from north to south across the equator in the morning, while Aqua passes south to north over the equator in the afternoon. The MODIS instrument has a viewing swath width of 2,330 km and views the entire surface of the Earth every one to two days. Its detectors measure 36 spectral bands between 0.405 and 14.385 μm , and it acquires data at three spatial resolutions: 250m, 500m, and 1,000m. The data products derived from MODIS observations describe features of the land, oceans and the atmosphere that can be used for studying processes and trends on local to global scales to improve our understanding of global dynamics and processes occurring on land, in the oceans, and in the lower atmosphere. MODIS plays a vital role in the development of validated, global, interactive Earth system models able to predict global change accurately enough to assist policy makers in making sound decisions concerning the protection of our environment.

Figure 3 shows an example of sea ice concentration (SIC) retrievals from MODIS observations as a proxy for GOES-R ABI. One is based on MODIS retrieved ice surface skin temperature, and the other is based on MODIS visible band reflectance at 0.64 μm . Both retrievals show similar results, with high sea ice concentration near the North Pole and lower values near the ice edges. This example shows that the ice concentration retrieval algorithm works for sea ice concentration retrieval using MODIS data.

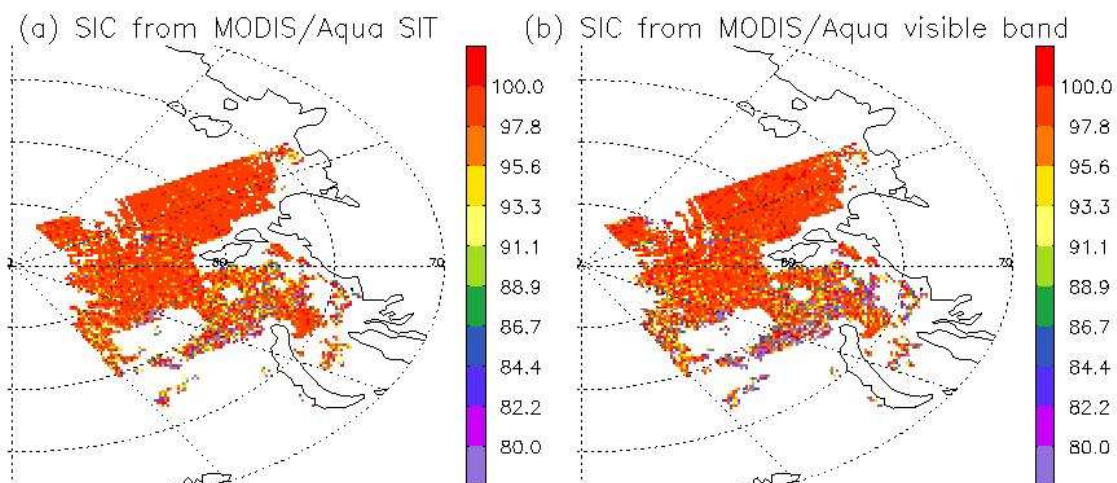


Figure 3. Sea ice concentration (%) retrieved from (a) MODIS Sea Ice Temperature (SIT), (b) MODIS visible band ($0.64 \mu\text{m}$) reflectance using the tie point algorithm on March 31st, 2006.

Figure 4 shows an example of ice concentration retrievals over the Great Lakes and inland waters from MODIS observations using the tie point algorithm based on MODIS visible band reflectance. The retrieved ice concentration agrees well with those observed from the MODIS true color image. This example shows that the tie point algorithm works for lake ice concentration retrieval using MODIS data.

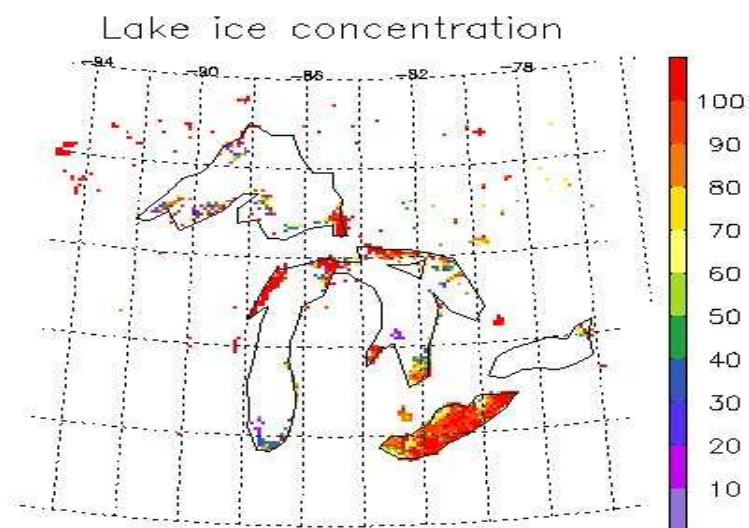


Figure 4. Lake ice concentration (%) with MODIS Aqua visible band ($0.64 \mu\text{m}$) data on February 24, 2008.

5.1.2 SEVIRI Data

SEVIRI is the primary payload of the MSG satellites, which have been a joint project between the European Space Agency and EUMETSAT (the European Organisation for the Exploitation of Meteorological Satellites) since 1977 (refer to http://www.eumetsat.int/home/Main/Access_to_Data/Meteosat_Image_Services/SP_1123237865326). SEVIRI measures reflected and emitted radiance in 11 spectral channels located between 0.6 μm and 14 μm with a nominal spatial resolution of 3 km at the sub-satellite point along with an additional broadband high-resolution visible (0.4-1.1 μm) channel that has 1 km spatial resolution. The full disk view allows frequent sampling, every 15 minutes, enabling monitoring of rapidly evolving events. The nominal coverage includes all of Europe, Africa and locations at which the elevation to the satellite is greater than or equal to 10° (Figure 5).

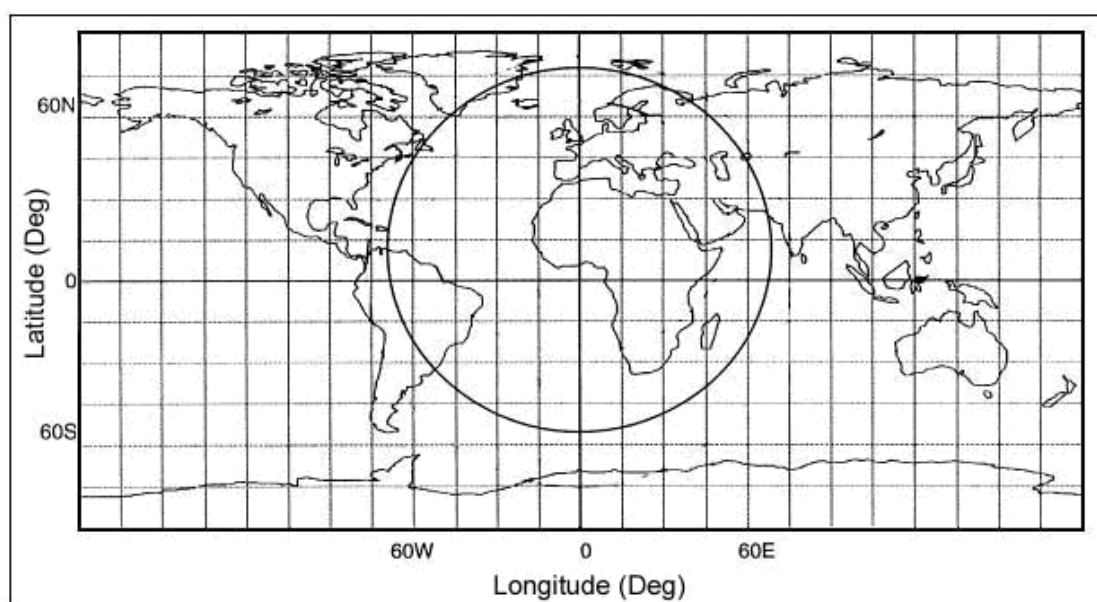


Figure 5. MSG Telecommunications coverage area.

Figure 6 shows an example of ice concentration retrievals over the Caspian Sea from SEVIRI observations using the tie point algorithm. One retrieval is based on SEVIRI retrieved ice surface temperature, and the other is based on SEVIRI visible band reflectance at 0.64 μm . Both retrievals show very similar results, with higher values over the northern part and lower values over the southern part. Comparison of the retrieved ice concentration to those observed from a satellite true color image show good agreement, which demonstrates that this ice concentration retrieval algorithm works for lake ice concentration retrieval using SEVIRI data.

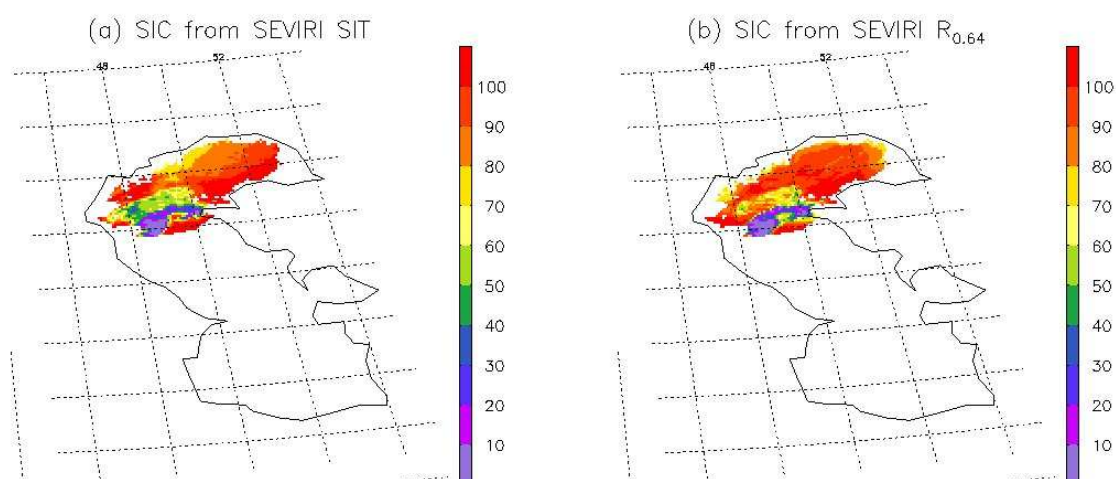


Figure 6. Lake ice concentration (%) retrieved from (a) SEVIRI Surface Ice Temperature (SIT), (b) SEVIRI visible band reflectance ($0.64 \mu\text{m}$) on January 27th, 2006.

5.2 Output from Simulated Inputs Data Sets

5.2.1 Precisions and Accuracy Estimates

The product measurement accuracy requirement for ice cover is a correct detection rate of 85%. The product measurement accuracy requirement for ice concentration is 10%, with a product measurement precision of 30%. Direct match ups and comparison between satellite retrieved ice cover and concentration and satellite true color images are made to gain qualitative results. Comparison of the retrieved products with ice cover and concentration from microwave observations provides quantitative results, with mean bias, standard deviation, and bias frequency distribution presented.

Future validations will include extensive comparisons and validations of satellite retrieved ice cover and concentration with those from microwave observations, ice charts of ice concentration at a spatial resolution of 25 km or higher, and satellite retrieved ice cover and concentration from the Thematic Mapper onboard Landsat 6 and 7 with a spatial resolution of 30 meters.

5.2.1.1 Comparison with the AMSR-E product

The AMSR-E instrument onboard Aqua is a twelve-channel, six-frequency, conically-scanning, passive-microwave radiometer system. It measures horizontally and vertically polarized microwave radiation (brightness temperatures) ranging from 6.9 GHz to 89.0 GHz. Spatial

resolution of the individual measurements varies from 5.4 km at 89 GHz to 56 km at 6.9 GHz. The AMSR-E instrument provides measurements of land, oceanic, and atmospheric parameters, including sea ice concentration, snow water equivalent, etc.

The AMSR-E Level-3 gridded product (AE_SI12) includes sea ice concentration mapped to a polar stereographic grid at 12.5 km spatial resolution. This dataset is used to compare with the sea ice concentration retrievals using MODIS as a proxy for GOES-R ABI data using the tie point algorithm.

Figure 7 shows an example of a comparison of sea ice concentration from the AMSR-E product and from MODIS. Both the product and the retrieval show similar patterns in the sea ice concentration, high values in the central Arctic and lower values towards the Barents Sea. The MODIS retrievals show more details in the central Arctic corresponding to leads in the sea ice. The MODIS retrievals also show lower sea ice concentration towards the open water. Although AMSR-E is not ground truth, statistical estimates of differences between these sea ice concentrations might provide helpful information for improving the retrieval algorithm. The MODIS sea ice concentrations were averaged for 11x11 pixels (native resolution is 1 km at the sub-satellite point) centered on the AMSR-E footprint (about 12 km nadir). For this specific case, the bias and standard deviation between AMSR-E and MODIS surface skin temperature (reflectance) based sea ice concentration are 2.8% (5.6%), and 4.1% (7.5%).

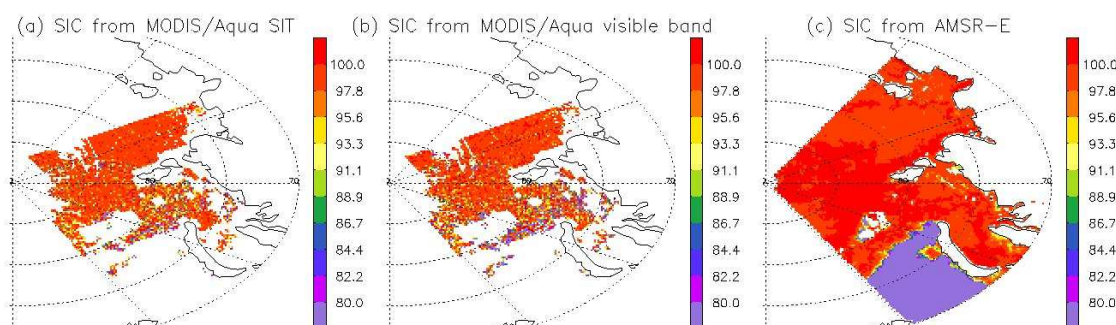


Figure 7. Sea ice concentration (SIC) (%) retrieved from (a) MODIS Sea Ice Temperature (SIT), (b) MODIS visible band reflectance, and (c) from Advanced Microwave Scanning Radiometer - Earth Observing System (AMSR-E) Level-3 gridded daily mean from NSIDC on March 31, 2006.

5.2.1.2 Comparison with the satellite true color images

Lake ice concentrations are also compared with satellite true color images for qualitative purposes. Though these comparisons cannot give quantitative results, it helps to show whether the retrieved ice cover and concentration have reasonable distributions.

Figure 8 shows an example of a comparison of retrieved lake ice concentration over the Caspian Sea with a satellite true color image. The lake ice concentration shows high values near shore,

and decreases southward until open water. The region between the fully ice covered region and open water shows gradually changing ice concentration, which is consistent with the observations from the satellite true color image.

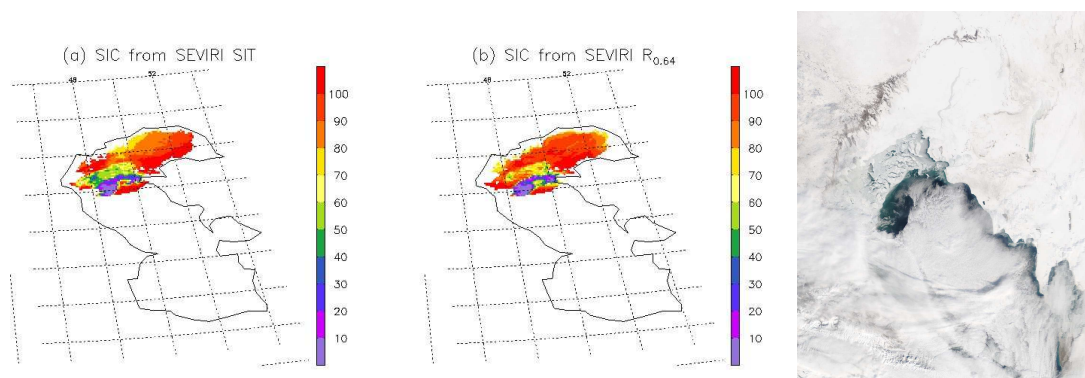


Figure 8. Lake ice concentration (%) retrieved from (a) SEVIRI Surface Ice Temperature (SIT), (b) SEVIRI visible band reflectance ($0.64 \mu\text{m}$), and (c) satellite true color image over the Caspian Sea on January 27, 2006.



Figure 9. Lake ice concentration (%) with MODIS Aqua data (left), MODIS true color image (middle), and ice concentration from AMSR-E (right) over the Great Lakes on February 24, 2008.

Figure 9 shows another example of a comparison of MODIS retrieved lake ice concentration with a satellite true color image. The lake ice cover shows good agreement with that inferred from the satellite true color image, as well as the distribution of ice concentration.

5.2.2 Error Budget

Retrieved ice cover concentration using MODIS data as a proxy over the Arctic on 41 days evenly distributed in four seasons and over the Great Lakes on a similar number of days are compared with the ice concentration product from AMSR-E as truth. A pixel is determined as

not ice covered as truth if the AMSR-E sea ice concentration is lower than 15%. Comparisons show that the correct detection ratio of ice cover is 87.6% (Table 5), which is higher than the required measurement accuracy for ice cover.

Table 8: Performance of ice cover product

Case Number Total pairs: 1576298	Sea/Lake ice cover determined from AMSR-E	Water surface determined from AMSR-E
Sea/Lake ice cover determined using this algorithm	1075124	
Water surface determined using this algorithm		305872
Correct detection ratio = $(1075124+305872)/1576298 = 87.6\%$		

A histogram of these two ice concentration differences is shown in Figure 10, and bias and standard deviation of these differences are shown in Table 6. Results show ice concentration retrievals using MODIS data as a proxy meet the ice cover and concentration accuracy and precision requirement, 10% and 30%, in comparison with the AMSR-E product as truth. Further tuning of this algorithm, including ice detection test thresholds, and preset parameter values will be carried out. Extensive validation will be done over sea and inland water. Also, quantitative validation of this algorithm will be conducted by comparing the derived ice cover and concentration with the ice chart product from a satellite instrument with a higher spatial resolution, like Landsat.

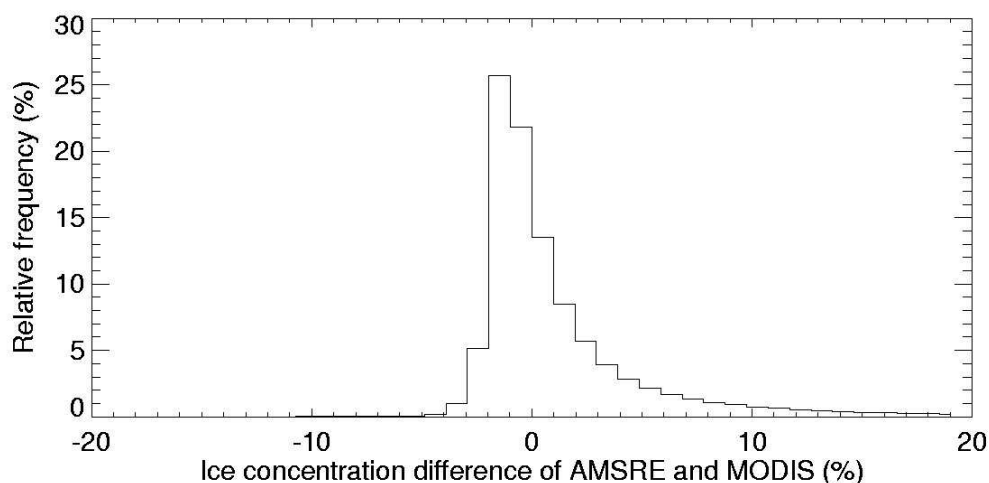


Figure 10. Frequency distribution of ice concentration difference between AMSRE product and retrievals using this algorithm based on a selection of 41 clear day MODIS data in four seasons in 2007 over the Arctic Ocean.

Table 9. Performance of retrieved ice concentration.

Ice concentration difference of AMSR-E product	Mean bias (%)	Standard Deviation (%)
--	---------------	------------------------

and MODIS product as proxy of GOES-R ABI		
Over Arctic Ocean	4.0	15.7
Over Great Lakes	-4.0	25.6
Required Measurement Accuracy	10	
Required Measurement Precision		30

6 Practical Considerations

6.1 Numerical Computation Considerations

This ice cover and concentration algorithm is implemented sequentially. The computation time is very economic.

6.2 Programming and Procedural Considerations

This ice cover and concentration algorithm requires spatial information distributions in a search window. Temporal information from previous observations is not necessary.

6.3 Quality Assessment and Diagnostics

The following procedures are recommended for diagnosing the performance of this algorithm.

- Check input data such as surface skin temperature and reflectance for all pixels.
- Monitor the products automatically with other products from different satellite, and real time in-situ observations.
- Periodically image the individual test results to look for artifacts or non-physical behaviors.
- Maintain a close collaboration with other teams, which use the output of this algorithm in their product generation.

6.4 Exception Handling

In addition to checking the validity of input data before running, this algorithm also checks for missing input variables values. In this case, a correspondent flag is set to indicate that no ice cover and concentration were produced for that pixel.

6.5 Algorithm Validation

This algorithm is validated using MODIS and SEVIRI data as proxy data. Bias and standard deviation of ice concentration are calculated using many cases. Results show that this algorithm will meet the MRD required accuracy. More extensive validation will be carried out using proxy data, such as MODIS, SEVIRI and other proxy data sets, over ocean and inland waters, in comparison with ice products from AMSR-E, ice charts, and satellite instruments with very high spatial resolution.

7 Assumptions and Limitations

The following sections describe limitations and assumptions in the current version of this algorithm.

7.1 Assumptions

The following assumptions have been made in developing and estimating the performance of this algorithm. The following list contains the current assumptions and proposed mitigation strategies.

1. Cloud mask eliminates all possible cloud contamination.
2. Land mask maps are available to identify different surface types.
3. Changes in reflectance/temperature in each search window are mainly caused by difference in ice concentration on the pixel level. Viewing angles in a search window do not change much considering the size of the search window. Pixels with 100% ice cover are the majority in a search window.

We assume that the sensor will meet its current specifications and that retrieved products from other teams will be accurate enough for this algorithm. This algorithm will be dependent on the following retrieved products:

- Surface skin temperature, and
- Visible channel reflectance.

As for sensitivity estimates, a source error of 0.5 K (0.01) in surface skin temperature (visible channel reflectance) leads to around 2% (2%) error in ice concentration, with the tie point ice surface skin temperature (visible reflectance) being 250 K (0.55).

7.2 Limitations

Limitations of this algorithm include:

1. Ice concentration is not retrieved if less than 10% of all pixels in a search window are covered by ice, in which the tie-point reflectance or surface temperature can not be determined. However, ice cover can still be identified. Quality flags are set in the final ice concentration product for this condition.
2. The assumption that 100% ice covered pixels are the majority in a search window can be violated under some conditions, when partially ice covered pixels are more than 100% ice covered pixels, which might lead to uncertainties in the final ice concentration estimations.

7.3 Pre-Planned Product Improvements

We will attempt to handle the limitations discussed in 6.2, given the uncertainties these limitations might cause in the final product.

This algorithm serves other applications. Its development is closely tied to the development and feedback from the other team algorithms. At this point, it is therefore difficult to predict what the future modifications will be. We intend to allow for feedback and to incorporate any suggestions from other teams to improve this algorithm.

8 References

Appel I., and J. A. Kenneth, 2002, Fresh water ice Visible/Infrared Imager/Radiometer Suite algorithm theoretical basis document, Version 5. SBRS document #: Y2404.

Bolsenga, S.J. 1983, Spectral reflectances of snow and fresh-water ice from 340 through 1100 nm. *J. Glaciology*, 29(102), 296-305.

Grenfell, T. C. and G. A. Maykut, 1977, The optical properties of ice and snow in the Arctic Basin, *J. Glaciol.*, 18, 445-63.

Hall D.K., G.A. Riggs, and V.V. Salomonson, 2001, Algorithm theoretical basis document for the MODIS snow and sea ice mapping algorithms.

Hall D.K., G.A. Riggs, and V.V. Salomonson, 2006, MODIS sea ice products user guide to collection 5.

Key, J., J. Collins, C. Fowler, and R. Stone, 1997, High-latitude surface temperature estimates from thermal satellite data. *Remote Sensing Environ.*, 61, 302-309.

Lindsay, R. W., and D. A. Rothrock 1995, Arctic sea ice leads from advanced very high resolution radiometer images, *J. Geophys. Res.*, 100, 4533-4544.

Riggs G.A., D.K. Hall, and S.A. Ackerman, 1999, Sea ice extent and classification mapping with the Moderate Resolution Imaging Spectroradiometer Airborne Simulator. *Remote Sensing of Environ.*, 68, 152-163.

Schmit, Timothy J., Mathew M. Gunshor, W. Paul Menzel, James J. Gurka, Jun Li, A. Scott Bachmeier, 2005: INTRODUCING THE NEXT-GENERATION ADVANCED BASELINE IMAGER ON GOES-R. *Bull. Amer. Meteor. Soc.*, 86, 1079-1096